

# QCD near the Light Cone

H. W. L. Naus<sup>a,b</sup>, H. J. Pirner<sup>a</sup>, T. J. Fields<sup>a,c</sup>, and J. P. Vary<sup>a,c</sup>

*<sup>a</sup>Institute for Theoretical Physics, University of Heidelberg*

*Philosophenweg 19, 69120 Heidelberg, Germany*

*<sup>b</sup>Institute for Theoretical Physics, University of Hannover*

*Appelstr. 2, 30167 Hannover, Germany*

*<sup>c</sup>Department of Physics and Astronomy, Iowa State University*

*Ames, IA 50011*

(June 18, 2021)

## Abstract

Starting from the QCD Lagrangian, we present the QCD Hamiltonian for near light cone coordinates. We study the dynamics of the gluonic zero modes of this Hamiltonian. The strong coupling solutions serve as a basis for the complete problem. We discuss the importance of zero modes for the confinement mechanism.

Typeset using REVTeX

## I. INTRODUCTION

The formulation of light front QCD is one of the most innovative enterprises in recent theoretical hadron physics. It resumes the pioneering efforts of the seventies in the parton model [1,2]. Its intention is to connect the successful parton model at large resolution  $Q^2$  with the constituent quark picture of hadrons appearing in spectroscopy. The new start [3] is not without a knowledge of the problems which have been experienced in the first works. It is well documented that renormalization in Hamiltonian field theories is, with currently available methods, more cumbersome than in covariant descriptions. A naive gauge fixing procedure on the light front leads to an easy resolution of Gauss' Law. However, this naive method is not correct – the correct method involves so-called ‘zero mode’ degrees of freedom dependent on the transverse coordinates. These zero modes cannot be gauged away, and become an integral part of the dynamics. In addition we expect that the nontrivial vacuum structure evident from equal time quantization brings new induced couplings into the light front Hamiltonian.

Our investigation concentrates on the role of the zero mode fields. We start from the near light front frame advocated by the St. Petersburg and Erlangen groups [4,5] and introduce a finite volume ( $L \times L \times L$  in the spatial directions), thereby controlling possible infrared singularities. This choice of coordinate system involves quantization on a space-like surface, which makes it easier to relate the occurring phenomena to equal time physics. However, all the usual complexities of negative energy states and nontrivial vacua are also present.

An axial gauge is natural in the infinite momentum frame: the axis of motion singles out a preferred direction. The chosen gauge  $\partial_- A_- = 0$  is actually a variant of the axial gauge, since the latter is incompatible with the boundary conditions. Consequences include the appearance and quantization of the zero-mode gauge fields  $a_-(x_\perp)$  which depend only on the two transverse coordinates and can be chosen color diagonal. The asymmetrical dependence of the zero modes on only the transverse coordinates coincides with the asymmetry of the space coordinates in this near light front frame. Explicitly, the light front spatial  $x^-$  direction

stems from mixing the former spatial  $x^3$  coordinate with the former time  $x^0$ .

The zero modes degrees of freedom appear in a transverse Hamiltonian which is coupled to three-dimensional dynamics via the fermions, transverse gauge fields and the light front Coulomb law. In the strong coupling limit the kinetic term of the transverse Hamiltonian becomes dominant and, in this limit, the Hamiltonian is identical to a Hamiltonian describing independent rotators at each lattice site. This is the starting point of our investigation. Using basis functions according to this dominant kinetic term, we make an expansion of the zero mode Hamiltonian. In the strong coupling basis we also evaluate the Coulomb term and find indications that the interaction of external sources is confining.

In Hamiltonian formulations quantized on the exact light front, the zero modes  $a_-(x_\perp)$  correspond to high energies. They are infinitely long wavelength excitations with respect to the spatial variable  $x^-$ , and, simultaneously, they are very short wavelength (ultraviolet) excitations with respect to the time variable  $x^+$ . Therefore some approaches [6] include the zero mode physics in their renormalization program, without explicitly solving their dynamics. In our approach of near light cone coordinates, the zero modes are independent degrees of freedom and retained after the solution of Gauss' Law, since they correspond to gauge invariant quantities (as evident in their role as eigenphases of the Polyakov loops). Resolution of the Gauss law constraint indeed does not permit the elimination of their conjugate momenta  $p^-(x_\perp)$ .

The existence of zero modes indicates that the local color charge of all external sources will be singlet – all hadronic bound states must be color singlets. This is the first requirement of color confinement. The second requirement for color confinement dictates that the interaction energy increases with increasing separation. To make a reliable calculation in this case, one has to know, besides the light front Coulomb potential, how gluon fields propagate in the 'background' field  $a_-(x_\perp)$  over large distances. It is argued that on a strongly coupled lattice the background field modifies the behavior of transverse plane gluon waves with color charge. Due to the fluctuations of the background they are limited to propagate over short distances. Thus they cannot cancel the linear confinement potential induced by

the gauge choice. In this way, the axial gauge supports confinement from the beginning and therefore seems to be the best starting point for QCD. However, confinement is not so obvious for neutral transverse gluon fields, whose two-dimensional longitudinal zero mode part has been eliminated in the procedure of solving the Gauss law constraint.

Light front gauge theories have been set up using the so-called near light front frame [4,5,7,8], which enables one to study the approach to the exact light front. The tilted coordinates are defined as

$$\begin{aligned} x^+ &= \frac{1}{\sqrt{2}} \left\{ \left( 1 + \frac{\eta^2}{2} \right) x^0 + \left( 1 - \frac{\eta^2}{2} \right) x^3 \right\} , \\ x^- &= \frac{1}{\sqrt{2}} (x^0 - x^3) . \end{aligned} \quad (1.1)$$

The transverse components  $x^1$  and  $x^2$  are unchanged;  $x^+$  is the new time coordinate and  $x^-$  is the remaining spatial coordinate. As finite quantization volume we will take a torus and its extension in  $x^-$ , as well as in  $x^1, x^2$  direction is  $L$ . The metric tensor reads

$$g_{\mu\nu} = \begin{pmatrix} 0 & 0 & 0 & 1 \\ 0 & -1 & 0 & 0 \\ 0 & 0 & -1 & 0 \\ 1 & 0 & 0 & -\eta^2 \end{pmatrix} , \quad g^{\mu\nu} = \begin{pmatrix} \eta^2 & 0 & 0 & 1 \\ 0 & -1 & 0 & 0 \\ 0 & 0 & -1 & 0 \\ 1 & 0 & 0 & 0 \end{pmatrix} , \quad (1.2)$$

where  $\mu, \nu = +, 1, 2, -$ . It defines the scalar product of two 4-vectors  $x$  and  $y$ :

$$\begin{aligned} x_\mu y^\mu &= x^- y^+ + x^+ y^- - \eta^2 x^- y^- - \vec{x}_\perp \vec{y}_\perp \\ &= x_- y_+ + x_+ y_- + \eta^2 x_+ y_+ - \vec{x}_\perp \vec{y}_\perp , \end{aligned} \quad (1.3)$$

where

$$\vec{x}_\perp \vec{y}_\perp = x^1 y^1 + x^2 y^2 . \quad (1.4)$$

Obviously, the exact light-cone is approached as the parameter  $\eta^2$  goes to zero. For non-zero  $\eta$ , the transition to the near light front coordinates from an equal time frame can be formally identified as a Lorentz boost combined with a linear transformation which avoids

time dependent boundary conditions [5], as required in the canonical formulation. The boost parameter  $\beta$  for this Lorentz transformation (in the  $x^3$  direction) is given by

$$\beta = \frac{1 - \eta^2/2}{1 + \eta^2/2}, \quad (1.5)$$

indicating that for  $\eta \rightarrow 0$  the relative velocity of the two frames  $v = \beta c \rightarrow c (\equiv 1)$ . This is connected to the interpretation of the near light front frame in terms of the infinite momentum frame. As discussed previously, the use of these near light front coordinates allows us to quantize the theory on a spacelike surface at equal light front time. This is important, as the ends of our ‘box’ are spacelike separated, and can thus exchange no information. Note the contrast to conventional light front coordinates, in which the ends of the ‘box’ are separated by a light-like interval which, in turn, implies that the surface of quantization contains points which can be causally connected.

The spectrum of massless partons  $p_\mu p^\mu = 0$  with transverse momentum  $p_\perp$  can be easily calculated from their dispersion relation which reads in the near light front coordinates

$$2p_- p_+ + \eta^2 (p_+)^2 - p_\perp^2 = 0. \quad (1.6)$$

In our coordinates,  $p_+$  is the energy variable (being conjugate to  $x^+$ ) and  $p_-$  is the longitudinal momentum variable. This dispersion relation has two  $p_+$  solutions, an upper branch  $p_{+,up}$  and a lower branch  $p_{+,down}$

$$p_{+,up/down} = -\frac{1}{\eta^2} \left( p_- \mp \sqrt{(p_-)^2 + \eta^2 p_\perp^2} \right). \quad (1.7)$$

In the limit of small  $\eta$ , Eq. (1.7) goes over into the conventional light front energy

$$p_{+,up} \rightarrow p_{+,lc} = p_\perp^2 / 2p_{-,lc}. \quad (1.8)$$

In Figure 1, we show these two branches together with the light front Hamiltonian  $p_{+,lc} = p_\perp^2 / 2p_{-,lc}$ . We have taken the maximum transverse momentum  $p_\perp = 1/a$ ,  $\eta = 0.1$ , and all energies and momenta are in units of  $1/a$ , where  $a$  is the lattice spacing. Note that negative momentum states correspond uniquely to negative energy states in the conventional

light front formalism, but with our choice of coordinates, this clean division no longer holds. However, it is true that for small  $\eta$ , the negative momentum states with positive energy are of very high energy, indeed. One possible procedure to find the momenta for regularization of these high energy states is to calculate the longitudinal momenta corresponding to a maximum absolute energy

$$-\frac{1}{\eta a} < p_+ < \frac{1}{\eta a}. \quad (1.9)$$

For  $p_\perp = 1/a$ , this cutoff corresponds to  $p_- = 0$  in  $p_{+,up/down}$  and renders the dispersion relation single-valued once again: a unique energy  $p_+$  corresponds to each momentum  $p_-$ .

Since we are finally interested in using  $p_{+,lc}$  as our effective Hamiltonian, the upper energy cutoff gives the minimal  $p_-$  momentum where this approximation still makes sense. When we use the expression in Eq. (1.8) for  $p_{+,lc}$  we obtain a minimal  $p_- = \eta/2a$ , resulting from our energy cutoff. To introduce an efficient light front effective theory, it is necessary to eliminate partons with negative  $p_-$  states with special attention to the partons with  $0 < p_- < \eta/2a$ . This procedure will not be discussed here, but we believe that this elimination is very important in order to obtain a constituent quark picture on the light front. We would further comment that our effective Hamiltonian approach discussed in the next chapter may provide a workable framework to include these high energy modes.

This paper is divided in six sections. In the next section we review the QCD Hamiltonian in the case of these tilted light front coordinates. In section 3 we give the solution to the zero mode sector in the strong and weak coupling approximations. A calculation of the ground state energy in the two site approximation is presented in section 4. Section 5 contains a discussion of confinement. Finally, we summarize in section 6.

## II. QCD HAMILTONIAN NEAR THE LIGHT FRONT

Canonical formulations of QED in the axial gauge and in the light front gauge have been developed in analogous ways – starting from the respective canonical Weyl gauges. After the

implementation of the Gauss law constraints, the resulting Hamiltonians appear to be rather similar [9]. Moreover, the QCD Hamiltonian in axial gauge representation has recently been derived [10]. Here we will outline the derivation of the near light front QCD Hamiltonian, which has been given by the Erlangen group [11] also. We restrict ourselves to the color gauge group  $SU(2)$  and dynamical gluons; only an external (fermionic) charge density  $\rho_m$  is considered here. General  $SU(N)$  results, including dynamical fermions, are given in the Appendix.

The Lagrangian in the near light front coordinate system reads

$$\mathcal{L} = \frac{1}{2}F_{+-}^a F_{+-}^a + \sum_{i=1,2} \left( F_{+i}^a F_{-i}^a + \frac{\eta^2}{2} F_{+i}^a F_{+i}^a \right) - \frac{1}{2} F_{12}^a F_{12}^a - \rho_m^a A_+^a, \quad (2.1)$$

where the color index  $a$  is summed from 1 to 3, and the transverse coordinates are labeled by  $i = 1, 2$ . We will also use the matrix notation; for example  $A_- = A_-^a \tau^a / 2$ , where the  $\tau^a$  are the  $SU(2)$  matrices. The field strength tensor contains the commutator of the gauge fields:

$$F_{\mu\nu} = \partial_\mu A_\nu - \partial_\nu A_\mu - ig[A_\mu, A_\nu], \quad (2.2)$$

with the coupling constant  $g$ .

The  $A_+^a$  coordinates have no momenta conjugate to them. As a consequence, the Weyl gauge  $A_+^a = 0$  is the most natural starting point for a canonical formulation. The canonical momenta of the dynamical fields  $A_-^a, A_i^a$  are given by

$$\begin{aligned} \Pi_-^a &= \frac{\partial \mathcal{L}}{\partial F_{+-}^a} = F_{+-}^a, \\ \Pi_i^a &= \frac{\partial \mathcal{L}}{\partial F_{+i}^a} = F_{-i}^a + \eta^2 F_{+i}^a. \end{aligned} \quad (2.3)$$

From this, we get the Weyl gauge Hamiltonian density

$$\mathcal{H}_W = \frac{1}{2} \Pi_-^a \Pi_-^a + \frac{1}{2} F_{12}^a F_{12}^a + \frac{1}{2\eta^2} \sum_{i=1,2} \left( \Pi_i^a - F_{-i}^a \right)^2. \quad (2.4)$$

We choose periodic boundary conditions in  $x^-$  and  $x_\perp$  on intervals of size  $[0, L]$ . Using the appropriate periodic delta functions, the quantization is straightforward. However, the

Hamiltonian has to be supplemented by the original Euler–Lagrange equation for  $A_+$  as constraints on the physical states

$$\begin{aligned} G^a(x_\perp, x^-)|\Phi\rangle &= \left(D_-^{ab}\Pi_-^b + D_\perp^{ab}\Pi_\perp^b + g\rho_m^a\right)|\Phi\rangle \\ &= \left(D_-^{ab}\Pi_-^b + G_\perp^a\right)|\Phi\rangle = 0, \end{aligned} \tag{2.5}$$

with the covariant derivatives

$$\begin{aligned} D_-^{ab} &= \partial_- \delta^{ab} + g f^{acb} A_-^c, \\ D_\perp^{ab} &= \partial_\perp \delta^{ab} + g f^{acb} A_\perp^c, \end{aligned} \tag{2.6}$$

where  $f^{acb}$  are the structure constants of  $SU(2)$ .

These equations are known as Gauss’ Law constraints. Since the Gauss’ Law operator commutes with the Hamiltonian

$$[G^a(x_\perp, x^-), H_W] = 0, \tag{2.7}$$

time evolution leaves the system in the space of physical states. Furthermore,  $H_W$  is invariant under time independent residual gauge transformations whose generator is closely connected to Gauss’ Law [10].

In order to obtain a Hamiltonian formulated in terms of unconstrained variables, thus rendered available for approximations without breaking local gauge invariance, one needs to resolve the Gauss’ Law constraint. This is an important step, since it frees us from implementing additional restrictions on operators or states. A Hamiltonian expressed in terms of unconstrained variables appears more complicated, but it is our belief that there is much to gain from this apparent increase in complexity.

Via unitary gauge fixing transformations [9,10] one indeed can achieve this resolution with respect to components of the chromo–electric field. These transformations render a Hamiltonian independent of the conjugate gauge fields. In other words, the latter become cyclic variables. Let us choose the ‘–’ (minus) components as the variables to be eliminated. Classically this would correspond to the light front gauge  $A_- = 0$ . However, this choice is



not legitimate for our setup in a finite box. Only the (classical) Coulomb light front gauge ( $\partial_- A_- = 0$ ) is compatible with gauge invariance and periodic boundary conditions. The reason is that  $A_-$  carries information on gauge invariant quantities, such as the eigenvalues of the spatial Polyakov (Wilson) loop

$$\mathcal{P}(x_\perp) = P \exp \left[ ig \int dx^- A_-(x_\perp, x^-) \right], \quad (2.8)$$

which can be written in terms of a diagonal matrix  $a_-(x_\perp)$

$$\mathcal{P}(x_\perp) = V \exp [igLa_-(x_\perp)] V^\dagger. \quad (2.9)$$

Thus, we obviously need to keep these ‘zero modes’  $a_-(x_\perp)$  as dynamical variables, while the other components of  $A_-$  are eliminated. The zero mode degrees of freedom are independent of  $x^-$  and, therefore, correspond to quantities with zero longitudinal momentum.

The unitary gauge fixing transformation can indeed be chosen in such a way that  $A_-$  becomes cyclic, apart from the zero modes mentioned [11]. In order to eliminate the conjugate momentum,  $\Pi_-$ , by means of Gauss’ Law, one needs to ‘invert’ the covariant derivative  $D_-$ . After the unitary transformation  $D_-$  simplifies significantly (compare to Eq. (2.6))

$$D_- \rightarrow d_- = \partial_- - ig[a_-, \quad], \quad (2.10)$$

where this is understood as an operator equation: e.g.  $D_- f \rightarrow d_- f = \partial_- f - ig[a_-, f]$  for arbitrary  $f$ . Now Gauss’ Law can be readily resolved: in the space of physical states one can make the replacement

$$\Pi_-(x_\perp, x_-) \rightarrow p_-(x_\perp) - (d_-^{-1}) G_\perp(x_\perp, y^-). \quad (2.11)$$

The inversion of  $d_-$  can be explicitly constructed in terms of its eigenfunctions, cf. [10,11]. The zero mode operator  $p_-(x_\perp)$  is also diagonal and  $p_-^3(x_\perp)$  is the conjugate momentum to  $a_-^3(x_\perp)$ . It has eigenvalue zero with respect to  $d_-$ , i.e.  $d_- p_- = 0$ , and is therefore not constrained.

The appearance of the zero modes also implies residual Gauss’ Law constraints. In the space of transformed physical states  $|\chi\rangle$ , they read

$$\int dx^- G_\perp^3 |\chi\rangle = \int dx^- \left( D_\perp^{3b} \Pi_\perp^b + g \rho_m^3 \right) |\chi\rangle = 0. \quad (2.12)$$

These two-dimensional constraints can be handled in full analogy to QED, since they correspond to the diagonal part of color space. This further gauge fixing in the  $SU(2)$  3-direction is done via another gauge fixing transformation, which leads to the Coulomb gauge representation in the transverse plane for the neutral fields. In other words, we eliminate the color neutral,  $x^-$ -independent, two-dimensional longitudinal gauge fields

$$a_\perp^\ell(x_\perp) = \frac{1}{L} \int dy^- dy_\perp d(x_\perp - y_\perp) \nabla_\perp \left( \nabla_\perp \cdot A_\perp^3(y_\perp, y^-) \right) \frac{\tau^3}{2}. \quad (2.13)$$

Here we use the periodic Greens function of the two dimensional Laplace operator

$$d(z_\perp) = -\frac{1}{L^2} \sum_{\vec{n} \neq \vec{0}} \frac{1}{p_n^2} e^{ip_n z_\perp}, \quad p_n = \frac{2\pi}{L} \vec{n}, \quad (2.14)$$

where  $\vec{n} = (n_1, n_2)$  and  $n_1, n_2$  are integers. The conjugate momenta of these fields,  $p_\perp^\ell(x_\perp)$ , are defined analogously. Resolution of the residual Gauss' Law allows one to replace them, in the sector of the transformed physical space  $|\Phi'\rangle$ , by the neutral chromo-electric field

$$e_\perp(x_\perp) = g \nabla_\perp \int dy^- dy_\perp d(x_\perp - y_\perp) \left\{ f^{3ab} A_\perp^a(y_\perp, y^-) \Pi_\perp^b(y_\perp, y^-) + \rho_m^3(y_\perp, y^-) \right\} \frac{\tau^3}{2}. \quad (2.15)$$

At this point it is convenient to introduce the unconstrained gauge fields and their conjugate momenta:

$$\begin{aligned} A'_\perp(x_\perp, x^-) &= A_\perp(x_\perp, x^-) - a_\perp^\ell(x_\perp), \\ \Pi'_\perp(x_\perp, x^-) &= \Pi_\perp(x_\perp, x^-) - \frac{1}{L} p_\perp^\ell(x_\perp). \end{aligned} \quad (2.16)$$

These relations turn out to be important for neutral gluon exchange; recall that the subtracted fields are diagonal in color space. Note that the physical degrees of freedom  $A'_\perp$  and  $\Pi'_\perp$  still contain  $(x_\perp, x^-)$ -independent, color neutral, modes. Therefore, there is a remnant of the local Gauss' Law constraints – the global condition

$$Q^3 |\Phi'\rangle = \int dy^- dy_\perp \left\{ f^{3ab} A_\perp^a(y_\perp, y^-) \Pi_\perp^b(y_\perp, y^-) + \rho_m^3(y_\perp, y^-) \right\} |\Phi'\rangle = 0. \quad (2.17)$$

The physical meaning of this equation is that the neutral component of the total color charge, including external matter as well as gluonic contributions, must vanish in the sector of physical states.

The final Hamiltonian density in the physical sector explicitly reads

$$\begin{aligned}
\mathcal{H} = & \text{tr} [\partial_1 A'_2 - \partial_2 A'_1 - ig[A'_1, A'_2]]^2 + \frac{1}{\eta^2} \text{tr} [\Pi'_\perp - (\partial_- A'_\perp - ig[a_-, A'_\perp])]^2 \\
& + \frac{1}{\eta^2} \text{tr} \left[ \frac{1}{L} e_\perp - \nabla_\perp a_- \right]^2 + \frac{1}{2L^2} p_-^{3\dagger}(x_\perp) p_-^3(x_\perp) \\
& + \frac{1}{L^2} \int_0^L dz^- \int_0^L dy^- \sum_{p,q,n} \frac{G'_{\perp qp}(x_\perp, z^-) G'_{\perp pq}(x_\perp, y^-)}{\left[ \frac{2\pi n}{L} + g(a_{-q}(x_\perp) - a_{-p}(x_\perp)) \right]^2} e^{i2\pi n(z^- - y^-)/L}, \quad (2.18)
\end{aligned}$$

where  $p$  and  $q$  are matrix labels for rows and columns,  $a_{-q} = (a_-)_{qq}$  and the prime indicates that the summation is restricted to  $n \neq 0$  if  $p = q$ . The operator  $G'_\perp(x_\perp, x^-)$  is defined as

$$G'_\perp = \nabla_\perp \Pi'_\perp + gf^{abc} \frac{\tau^a}{2} A'^b_\perp \left( \Pi'^c_\perp - \frac{1}{L} e^c_\perp \right) + g\rho_m. \quad (2.19)$$

In Table 1 we show the number of degrees of freedom for the different stages of the gauge fixing procedure. In order to count, we discretize configuration space as  $N^3$  sites. Constraints of course reduce the number of independent variables and are therefore subtracted. Originally there are three vector components of the gluon field in three colors at each site. Gauss' law represents three (color) constraints at each site. After the first unitary transformation we arrive at a intermediate Hamiltonian which is not explicitly given in the text. The number of degrees of freedom as well as the number of constraints have been reduced. Note that the residual Gauss law is two-dimensional and color neutral. Finally, we arrive at a formulation where there is only one global constraint left. Concomitantly, the final  $A'_\perp$  still contains the global color neutral zero mode which has not been subtracted (cf. Eqs. (2.13, 2.14)). Thus, one explicitly sees that the number of independent unconstrained degrees of freedom is  $6N^3$  at *any* stage of the formal development.

TABLES

TABLE I. Counting the degrees of freedom in the  $SU(2)$  Hamiltonians

<b>Original <math>\mathcal{H}</math></b>	
$A_1^a, A_2^a, A_-^a(x_\perp, x_-)$ :	$3 * 3 * N^3$
Gauss' law constraints:	$-3 * N^3$
	-----
	$6N^3$
<b>Intermediate <math>\mathcal{H}</math></b>	
$A_1^a, A_2^a(x_\perp, x_-)$ :	$2 * 3 * N^3$
Zero modes $a_-^3(x_\perp)$ :	$N^2$
Residual Gauss' law constraints:	$-N^2$
	-----
	$6N^3$
<b>Final <math>\mathcal{H}</math></b>	
$A_1^a, A_2^a(x_\perp, x_-)$ :	$2 * 3 * N^3 - (N^2 - 1)$
Zero modes $a_-^3(x_\perp)$ :	$N^2$
Global neutrality constraint:	$-1$
	-----
	$6N^3$

The formulation of axial gauge near light front QCD for  $SU(2)$  gauge fields is complete at this point. For details of the rather subtle derivation we refer to original references [10,11]. See also [12] for a pedagogical review and [13] for a critical discussion focusing on topological aspects. In [14] the method using unitary transformations has been applied to QED quantized on the exact light cone. The above Hamiltonian already is rather complex and nonlocal, just as the most familiar example of a gauge fixed theory, Coulomb gauge QED. Despite the complexity it serves as a promising starting point for further studies since approximations can be made without breaking local gauge invariance.

### III. ZERO MODE DYNAMICS

The principal advantage of an exact light front formulation is the apparent triviality of the ground state which simplifies calculations of the hadron spectrum. The light front vacuum, however, is not guaranteed to be trivial in the zero mode sector. In using the near light front coordinate system, we can study the complex zero mode structure influencing the dynamics of long distances. The zero mode sector in light front physics differs from equal time Hamiltonian physics where the long range physics is low energy physics. As can be seen from the dispersion relation for massless particles on the light front,  $p_+ = \frac{p_1^2}{2p_-}$ , soft modes (states with small momenta) become high energy states. In this way, high energy physics becomes tied to long range physics, contrary to the equal time formulation. This physics appears in deep inelastic scattering at small scaling variable and is related to the long distance features of the proton. We will focus on the zero mode sector in order to try to acquire some insight into its dynamics. Therewith we hope to obtain a sound basis for further numerical studies.

From the comparison of abelian and non-abelian theories, striking differences show up in the zero mode sector. Recently, in the equal time formalism, the zero mode sector in QCD has been claimed to be relevant for the confinement phenomenon [15]. On the level of approximations and restrictions followed below, the formal differences between light front

and equal time approach are rather small and, consequently, results and methods are similar.

In this work we do not restrict ourselves to the strong coupling approximation. We will, however, start with the strongly coupled theory to define our set of basis functions. As before, we will restrict ourselves to  $SU(2)$  without matter – pure gluonic Yang-Mills theory. It already has the typical non-abelian features such as the Coulomb term which explicitly contains the zero modes in the denominator and the non-standard kinetic energy for the zero modes.

The zero mode degrees of freedom couple to the three-dimensional gluon fields via the second term in  $\mathcal{H}$  shifting the longitudinal momenta of the transverse gluon fields (Eq. (2.18)). They affect the Coulomb term and the two-dimensional electric fields  $e_\perp$ . The latter coupling is typical for the light front and is absent in the equal time case. We neglect these couplings and consider the pure zero mode Hamiltonian

$$h = \int d^2x \left[ \frac{1}{2L} p_-^{3\dagger}(x_\perp) p_-^3(x_\perp) + \frac{L}{2\eta^2} (\nabla_\perp a_-^3(x_\perp))^2 \right]. \quad (3.1)$$

This Hamiltonian is obtained from Eq. (2.18) with only the zero mode  $a_-^3$  and its conjugate momentum retained, and an integration over the longitudinal variable. We recognize ‘electric’ and ‘magnetic’ contributions in  $h$ , the zero mode Hamiltonian – the first and second term, respectively. The light front variables mix the ordinary spatial and time variables so the labeling above is to be understood in analogy with the equal time Hamiltonian.

Even at this level of approximation, this zero mode Hamiltonian differs from the corresponding one in QED. The reason is the hermiticity defect of the canonical momentum:  $p_-^\dagger \neq p_-$ . This might seem to be a strange property for a momentum operator, but is perfectly allowable, in analogy with the naive radial Schrödinger momentum operator which is also non-Hermitian.

For notational simplicity, we now omit the color index and work with the Schrödinger representation of Eq. (3.1)

$$h = \int d^2x_\perp \left[ -\frac{1}{2L} \frac{1}{J(a_-(x_\perp))} \frac{\delta}{\delta a_-(x_\perp)} J(a_-(x_\perp)) \frac{\delta}{\delta a_-(x_\perp)} + \frac{L}{2\eta^2} (\nabla_\perp a_-(x_\perp))^2 \right], \quad (3.2)$$

where  $J(a_-)$  is the Jacobian and equals the Haar measure of  $SU(2)$

$$J(a_-(x_\perp)) = \sin^2\left(\frac{gL}{2}a_-(x_\perp)\right). \quad (3.3)$$

The Jacobian is connected to the hermiticity defect of  $p_-$ ; they stem from the gauge fixing procedure taking into account the curvilinear coordinates. The measure also appears in the integration volume element for calculating matrix elements. For ease of calculation, we introduce dimensionless variables

$$\varphi(x_\perp) = \frac{gL}{2}a_-(x_\perp), \quad (3.4)$$

in which Hamiltonian and Jacobian respectively read

$$h = \int d^2x_\perp \left[ -\frac{g^2L}{8} \frac{1}{J(\varphi(x_\perp))} \frac{\delta}{\delta\varphi(x_\perp)} J(\varphi(x_\perp)) \frac{\delta}{\delta\varphi(x_\perp)} + \frac{2}{\eta^2 g^2 L} (\nabla_\perp \varphi(x_\perp))^2 \right], \quad (3.5)$$

$$J(\varphi(x_\perp)) = \sin^2(\varphi(x_\perp)). \quad (3.6)$$

As in earlier approaches, see e.g. [17],  $\varphi$  will be treated as a compact variable,  $0 \leq \varphi < \pi$ .

At this stage it is necessary to appeal to the physics of the infinite momentum frame to factorize the reduced true energy  $h_{\text{red}}$  and the Lorentz boost factor  $\frac{\gamma}{\sqrt{2}} = \frac{1}{2\eta}$ , since essentially  $h$  is a light front energy, and it is well known how these behave under a Lorentz transformation. We rewrite

$$h = \frac{1}{2\eta} h_{\text{red}}, \quad (3.7)$$

with

$$h_{\text{red}} = \int d^2x_\perp \left[ -\frac{g^2L\eta}{4} \frac{1}{J} \frac{\delta}{\delta\varphi} J \frac{\delta}{\delta\varphi} + \frac{4}{g^2L\eta} (\nabla_\perp \varphi)^2 \right]. \quad (3.8)$$

It should be noted that the coefficients of the two terms are reciprocals of each other.

Since the integral over transverse coordinates can contain arbitrarily small wavelengths, we have to regularize the above Hamiltonian  $h_{\text{red}}$ . We do this by introducing a lattice to evaluate the transverse integral. The lattice vector  $\vec{b}$  numbers the lattice sites, and  $\vec{e}_1$

and  $\vec{\varepsilon}_2$  are the two unit vectors on the two-dimensional lattice. In order to have standard commutation relations on the lattice the derivative on the lattice becomes  $\frac{\delta}{\delta\varphi_{\vec{b}}} = \frac{\delta}{\delta\varphi(x_{\perp})}a^2$ . We further explicitly pull out the dependence on the lattice cutoff by defining a new reduced Hamiltonian  $\hat{h}_{\text{red}}$  and substituting  $\eta = \frac{1}{\sqrt{2}}aM$ , where  $M$  is a typical hadronic mass (see, e.g. [16]):

$$h = \frac{1}{2\eta a} \hat{h}_{\text{red}}, \quad (3.9)$$

with

$$\hat{h}_{\text{red}} = \sum_{\vec{b}} \left\{ -\frac{g^2 LM}{4\sqrt{2}} \frac{1}{J} \frac{\delta}{\delta\varphi_{\vec{b}}} J \frac{\delta}{\delta\varphi_{\vec{b}}} + \left( \frac{4\sqrt{2}}{g^2 LM} \right) \sum_{\vec{\varepsilon}} (\varphi_{\vec{b}} - \varphi_{\vec{b}+\vec{\varepsilon}})^2 \right\}. \quad (3.10)$$

Since the effective coupling constant,

$$g_{\text{eff}}^2 = \frac{g^2 LM}{4\sqrt{2}}, \quad (3.11)$$

contains the large factor  $LM$ , the product of lattice size in the longitudinal direction and the hadron mass, a strong coupling approach seems to be a good starting point.

We separate the Hamiltonian into electric and magnetic contributions:

$$\hat{h}_{\text{red}} = \sum_{\vec{b}} \hat{h}_{\vec{b}}^e + \sum_{\vec{b}} \hat{h}_{\vec{b}}^m, \quad (3.12)$$

where

$$\hat{h}_{\vec{b}}^e = -g_{\text{eff}}^2 \frac{1}{J} \frac{\delta}{\delta\varphi_{\vec{b}}} J \frac{\delta}{\delta\varphi_{\vec{b}}}, \quad (3.13)$$

and

$$\hat{h}_{\vec{b}}^m = \frac{1}{g_{\text{eff}}^2} \sum_{\vec{\varepsilon}} (\varphi_{\vec{b}} - \varphi_{\vec{b}+\vec{\varepsilon}})^2. \quad (3.14)$$

Note that we do not introduce ‘radial wave functions’ nor effective potentials as in [10,15]. For each lattice site  $\vec{b}$ , the electric part of the Hamiltonian  $\hat{h}_{\vec{b}}^e$  (the kinetic energy) has the Gegenbauer polynomials  $C_{n_{\vec{b}}}(\varphi_{\vec{b}})$  as eigenfunctions:

$$\hat{h}_{\vec{b}}^e C_{n_{\vec{b}}}(\varphi_{\vec{b}}) = g_{\text{eff}}^2 n_{\vec{b}}(n_{\vec{b}} + 2) C_{n_{\vec{b}}}(\varphi_{\vec{b}}), \quad (3.15)$$



with

$$C_{n_{\vec{b}}}(\varphi_{\vec{b}}) = \sqrt{\frac{2}{\pi}} \left\{ \frac{\sin((n_{\vec{b}} + 1)\varphi_{\vec{b}})}{\sin \varphi_{\vec{b}}} \right\}, \quad (3.16)$$

and

$$\int_0^\pi J(\varphi) C_n(\varphi) C_m(\varphi) d\varphi = \delta_{nm}. \quad (3.17)$$

The strong coupling wave functions of the full transverse lattice are product states characterized by a set of quantum numbers  $\{n\} = \{n_{\vec{b}}\}$ ,

$$\Psi_{\{n\}}(\varphi) = \prod_{\vec{b}} C_{n_{\vec{b}}}(\varphi_{\vec{b}}). \quad (3.18)$$

These functions form a complete and orthonormal basis for the zero mode sector. They satisfy the energy eigenvalue equation

$$\sum_{\vec{b}} \hat{h}_{\vec{b}}^e \Psi_{\{n\}}(\varphi) = g_{\text{eff}}^2 \sum_{\vec{b}} n_{\vec{b}}(n_{\vec{b}} + 2) \Psi_{\{n\}}(\varphi). \quad (3.19)$$

The ground state in this limit corresponds to all  $n_{\vec{b}} = 0$  – a constant wave function

$$\Psi_{\{0\}}(\varphi) = \prod_{\vec{b}} \sqrt{\frac{2}{\pi}}, \quad (3.20)$$

and the ground state energy is zero

$$E_0 = 0. \quad (3.21)$$

The first excited energy level is  $N_{\perp}^2$ -fold degenerate - an excitation at a single lattice point

$$\Psi_{\{1\}}(\varphi) = \sqrt{\frac{2}{\pi}} \frac{\sin(2\varphi_{\vec{b}})}{\sin \varphi_{\vec{b}}} \prod_{\vec{b}' \neq \vec{b}} \sqrt{\frac{2}{\pi}}. \quad (3.22)$$

In strong coupling this level is separated by a large amount from the ground state energy

$$E_1 = 3g_{\text{eff}}^2. \quad (3.23)$$

So far our results are equivalent to those of [15] to within re-definitions of wave functions and integration measures. In [17] weak coupling variational solutions for the full  $SU(2)$  lattice

Hamiltonian are given. Furthermore, studies in (1+1)–dimensional Yang-Mills theory [18] give formal extensions to construct wave functions for  $SU(N)$  gauge theories.

The magnetic term of the Hamiltonian couples nearest neighbor lattice points. In the strong coupling limit its contribution may be obtained perturbatively (as it has the coefficient  $1/g_{\text{eff}}^2$ ) by evaluating it with the basis function of the ground state. The result of this is

$$\langle \Psi_{\{0\}} | \sum_{\vec{b}} h_{\vec{b}}^m | \Psi_{\{0\}} \rangle = \frac{1}{g_{\text{eff}}^2} \left( \frac{\pi^2}{6} - 1 \right) \cdot (2N_{\perp}^2). \quad (3.24)$$

Since this energy is proportional to  $N_{\perp}^2 = (L/a)^2$  and  $g_{\text{eff}}^2$  grows linearly with  $L$ , this part of the zero mode dynamics represents a negligible surface effect for the three–dimensional system in the strong coupling approximation.

Next, we discuss the weak coupling limit  $g^2 \rightarrow 0$ . In this case we can simplify the kinetic term of the Hamiltonian by defining new variables  $\alpha_{\vec{b}}$ :

$$\alpha_{\vec{b}} = \frac{\varphi_{\vec{b}}}{\kappa g}, \quad (3.25)$$

with  $8\kappa^2 = \sqrt{2}LM$ . Then the reduced Hamiltonian becomes:

$$\hat{h}_{\text{red}} = \sum_{\vec{b}} \frac{-1}{\sin^2(\kappa g \alpha_{\vec{b}})} \frac{\partial}{\partial \alpha_{\vec{b}}} \sin^2(\kappa g \alpha_{\vec{b}}) \frac{\partial}{\partial \alpha_{\vec{b}}} + \sum_{\vec{b}, \vec{\varepsilon}} (\alpha_{\vec{b}}(\vec{b}) - \alpha_{\vec{b}+\vec{\varepsilon}})^2. \quad (3.26)$$

Expanding this for small  $g$ , we obtain

$$\hat{h}_{\text{red}} = \sum_{\vec{b}} \left\{ - \left( \frac{\partial^2}{\partial \alpha_{\vec{b}}^2} + \frac{2}{\alpha_{\vec{b}}} \frac{\partial}{\partial \alpha_{\vec{b}}} \right) + \sum_{\vec{\varepsilon}} (\alpha_{\vec{b}} - \alpha_{\vec{b}+\vec{\varepsilon}})^2 \right\}. \quad (3.27)$$

The eigensolutions of this Hamiltonian are known to be spin waves. Going over to Fourier momentum representation,

$$\alpha_{\vec{b}} = \sum_{\vec{k}} e^{i\vec{k}\vec{b}} R_{\vec{k}}, \quad (3.28)$$

with  $k_i = 2\pi n_i / N_{\perp} a$  and  $n_i = 0, \pm 1, \pm 2, \dots$  we have

$$\hat{h}_{\text{red}} = \sum_{\vec{k}} \left\{ - \left( \frac{\partial^2}{\partial R_{\vec{k}}^2} + \frac{2}{R_{\vec{k}}} \frac{\partial}{\partial R_{\vec{k}}} \right) + 4 \sum_{\vec{\varepsilon}} \sin^2 \frac{\vec{k}\vec{\varepsilon}}{2} R_{\vec{k}} R_{-\vec{k}} \right\}. \quad (3.29)$$

The eigensolutions  $\psi_K$  of  $\hat{h}_{\text{red}}$  in the weak coupling approximation are decoupled harmonic oscillators for each  $\vec{k}$ , with frequencies

$$\omega_k^2 = 4 \sum_{\vec{\varepsilon}} \sin^2 \frac{\vec{k}\vec{\varepsilon}}{2}. \quad (3.30)$$

Because of the ‘radial Laplacian’ it looks as if the eigenfunctions would have to vanish at the origin to be normalizable. However, as in the Schrödinger equation in three dimensions, the Jacobian  $J$  allows a constant wave function at the origin. Consequently, the eigenvalue of  $\psi_K$  is given by the sum over the modes:

$$\Omega_K = \sum_{\vec{k}} \sqrt{4 \sum_{\vec{\varepsilon}} \sin^2 \left( \frac{\vec{k}\vec{\varepsilon}}{2} \right)}, \quad (3.31)$$

which gives in the  $N_{\perp} \rightarrow \infty$  limit spin waves with  $\omega_{\vec{k}} = \sqrt{k_1^2 + k_2^2}$ .

In the weak coupling limit the zero mode Hamiltonian supports solutions similar to QED. The strong coupling limit, however, yields different results: ‘gluonic’ excitations are suppressed because of large energy gaps. This is due to the Jacobian, which can be traced back to non-abelian self interactions in the original Lagrangian.

#### IV. TWO-SITE TRUNCATION

We have obtained solutions in both the weak and strong coupling regime. We will now study the problem in the intermediate region. As an initial effort, we will not solve the problem for the full lattice. Rather, we will calculate with what is essentially a cluster expansion [16], and we will start with the simplest, two-site cluster, in which either site (or both) can be excited to high energy states. We will obtain the solution for the low-lying spectra of the system approximated as a low density of excitable two-site clusters. This method can be envisaged as the starting point of a more ambitious Hamiltonian based renormalization group technique, like the contractor renormalization group method (CORE) [19], or [20].

We handle the calculation of the energies via an effective Hamiltonian method. We work in the representation of the strong coupling solution of  $\hat{h}_b^e$  and divide the two-site subspace into a  $P$  and  $Q$  space, such that  $P + Q = 1$  with

$$\begin{aligned}
P &= \{|0, 0\rangle\}, \\
Q &= \{|n, m\rangle; n, m \neq 0, 0\},
\end{aligned}
\tag{4.1}$$

where  $n, m$  represent the indices of the Gegenbauer polynomials. Note that we have picked our  $P$  space as the strong coupling two-site ground state. Then the two-site energy  $E_2$  is given by the non-perturbative solution of the Hamiltonian in Eq. (3.12), truncated to two lattice sites. Explicitly, this Hamiltonian is:

$$\hat{h}_2 = \hat{h}^e + \hat{h}^m, \tag{4.2}$$

with

$$\hat{h}^e = -g_{\text{eff}}^2 \left\{ \frac{1}{J} \frac{\delta}{\delta\varphi_1} J \frac{\delta}{\delta\varphi_1} + \frac{1}{J} \frac{\delta}{\delta\varphi_2} J \frac{\delta}{\delta\varphi_2} \right\}, \tag{4.3}$$

and

$$\hat{h}^m = \frac{1}{g_{\text{eff}}^2} (\varphi_1 - \varphi_2)^2, \tag{4.4}$$

where the subscripts label the sites.

Within the effective Hamiltonian method, the two-site energy is given by (see, for example [21]):

$$E_2 = P\hat{h}_2P + P\hat{h}_2Q \frac{1}{E_2 - Q\hat{h}_2Q} Q\hat{h}_2P. \tag{4.5}$$

The self-consistent solutions of this equation provide the low-lying spectra in this method.

The strong coupling basis states are eigenstates of  $\hat{h}^e$ :

$$\hat{h}^e |n, m\rangle = g_{\text{eff}}^2 \{n(n+2) + m(m+2)\} |n, m\rangle. \tag{4.6}$$

Thus, the non-trivial matrix elements are those of  $\hat{h}^m$ , and are of the form

$$\langle n, m | (\varphi_1 - \varphi_2)^2 | n', m' \rangle. \tag{4.7}$$

Although our states are two-site states, the operators appearing in the matrix elements are simple one-site operators, and thus we can consider the states to be products of one-site

states. This reduces the evaluation to sums and products of one-site matrix elements, which are given as:

$$\begin{aligned}
\langle n|\varphi|n'\rangle &= \frac{\pi}{2} && \text{for } n = n' \\
\langle n|\varphi|n'\rangle &= \begin{cases} \frac{2}{\pi} \left( \frac{1}{(n+n'+2)^2} - \frac{1}{(n-n')^2} \right) & \text{for } n + n' = \text{odd} \\ 0 & \text{for } n + n' = \text{even}, n \neq n' \end{cases} \\
\langle n|\varphi^2|n'\rangle &= \begin{cases} \frac{2}{\pi} \left[ \frac{\pi^3}{6} - \frac{\pi}{[2(n+1)]^2} \right] & \text{for } n = n' \\ \frac{2}{\pi} \left\{ \pi(-1)^{n+n'} \left[ \frac{1}{(n-n')^2} - \frac{1}{(n+n'+2)^2} \right] \right\} & \text{for } n \neq n'. \end{cases} \quad (4.8)
\end{aligned}$$

Before performing any numerical calculation with the effective Hamiltonian, it will be illuminating to investigate the strong and weak coupling limits of this theory.

In the strong coupling limit we expect to obtain the result of perturbation theory in  $1/g_{\text{eff}}$ . The energy in this limit is easily calculated:

$$E_2 = \langle 0, 0 | \hat{h}^m | 0, 0 \rangle = \frac{1}{g_{\text{eff}}^2} \left\{ \langle 0 | \varphi^2 | 0 \rangle - 2 (\langle 0 | \varphi | 0 \rangle)^2 \right\} = \frac{1}{g_{\text{eff}}^2} \left( \frac{\pi^2}{6} - 1 \right). \quad (4.9)$$

In the weak coupling limit we can solve the Schrödinger equation for two neighboring sites - the Hamiltonian will simply be the two-site version of the earlier spin wave Hamiltonian, Eq. (3.27). We call the respective variables  $\alpha_{\vec{b}_1} = x$  and  $\alpha_{\vec{b}_2} = y$ , then we have to find the eigenenergies of the Hamiltonian:

$$\hat{h}_{\text{red}} = - \left( \frac{\partial^2}{\partial x^2} + \frac{2}{x} \frac{\partial}{\partial x} \right) - \left( \frac{\partial^2}{\partial y^2} + \frac{2}{y} \frac{\partial}{\partial y} \right) + (x - y)^2. \quad (4.10)$$

It should be noted that this Hamiltonian is invariant under  $x \leftrightarrow y$ , and thus the eigenfunctions  $\Psi_2(x, y)$  can be chosen to be symmetric under the interchange of  $x$  and  $y$  ( $\Psi_{2s}(x, y)$ ), or antisymmetric under the interchange of  $x$  and  $y$  ( $\Psi_{2a}(x, y)$ ). Each of these symmetric or antisymmetric sets of solutions form a ‘tower’ of excitations. The first symmetric excited state becomes degenerate with the ground state of the original problem in the weak coupling limit, and the first antisymmetric state has a greater energy than the first symmetric state.

As usual one factorizes the wave function

$$\Psi_2(x, y) = \frac{1}{xy} \Phi_2(x, y), \quad (4.11)$$

resulting in the Schrödinger equation

$$\hat{h}_{\text{red}}\Phi_2(x, y) = \left\{ -\frac{\partial^2}{\partial x^2} - \frac{\partial^2}{\partial y^2} + (x - y)^2 \right\} \Phi_2(x, y). \quad (4.12)$$

The center-of-mass motion is then separated:

$$\Phi_2(x, y) = e^{iPR}\chi_2(r), \quad (4.13)$$

with  $R = (x + y)/2$  and  $r = x - y$ . The Hamiltonian corresponding to the relative motion ( $r$ ) is a simple radial harmonic oscillator:

$$(\hat{h}_{\text{red}})_r = -2\frac{\partial^2}{\partial r^2} + r^2. \quad (4.14)$$

The lowest states of the symmetric and antisymmetric ‘towers’ are solutions to this Hamiltonian. The energies of these states can be read directly from Eq. (4.14);  $E_{2s} = \sqrt{2}$ , and  $E_{2a} = 3\sqrt{2}$ , respectively, giving a energy gap between the states of  $2\sqrt{2}$ .

Thus, the results for the energy gaps of the low-lying states in the weak coupling limit are

$$\begin{aligned} E_{2s} - E_{\text{ground}} &= 0, \\ E_{2a} - E_{\text{ground}} &= 2\sqrt{2}. \end{aligned} \quad (4.15)$$

We now proceed to calculate the low-lying spectra via the effective Hamiltonian method. In the numerical calculations, we cannot keep all states in the  $Q$  space – our choice is to cut at a high two-site energy, calculate  $E_2$ , then increase the size of the  $Q$  space to check for convergent results. This procedure was carried out for each choice of coupling constant  $g_{\text{eff}}$ , and the typical number of two-site states kept in the  $Q$  space at convergence was about 300.

The numerical solution of Eq. (4.5) for  $E_2$  is given in Figure 2. In the strong coupling limit (large  $g_{\text{eff}}^2$ ) the large gaps in energy are evident, and the numbers agree with the unperturbed energy of the states, given in Eq. (4.6). In this same limit, the slope of the ground state energy as a function of the inverse square coupling agrees with the analytic

calculation of Eq. (4.9). In the weak coupling limit, the results for the gap energies were Richardson extrapolated for the  $1/g_{\text{eff}}^2 \rightarrow \infty$  limit. This extrapolation matched the analytical results of Eq. (4.15) to five significant figures. Thus, we have obtained two-site solutions for the entire range of coupling which agreed with analytic results in the weak and strong coupling limits.

It is remarkable that we succeeded a one-dimensional strong coupling basis throughout the range of coupling strengths. Results for the spectra of  $N$ -sites are straightforwardly obtained as long as the number of excited two-site clusters is small compared with  $N/2$ . This is the ‘low density’ approximation.

## V. EFFECT OF ZERO MODES ON CONFINEMENT

In order to study the confinement problem, we start with the assumption that the three-dimensional gauge Hamiltonian can be treated in a weak coupling approximation with small gauge coupling  $g^2$ , whereas the physics of the two-dimensional zero mode subsystem can be obtained in a strong coupling approximation for  $g_{\text{eff}}^2 = \frac{g^2 LM}{4\sqrt{2}}$ . We will see that the asymmetric treatment of transverse and longitudinal spatial coordinates has effects, which go beyond the violation of rotational symmetry in strong coupling lattice gauge theory. They are connected with the procedure of initially choosing an axial gauge in three dimensions and then letting a two-dimensional Coulomb gauge follow. One advantage of this approach is that the dynamical role played by the zero modes becomes particularly illuminating. The zero modes preserve the axial linear confinement in first order perturbation theory. Thus, we argue that already at the level of the zero mode sector of  $SU(2)$  pure glue QCD we see evidence for confinement.

Let us demonstrate the usefulness of the basis functions obtained in the strong coupling approximation, cf. Eq. (3.16), by considering matrix elements of the Coulomb term. In terms of the variables  $\varphi$  defined on a discretized transverse space the Coulomb potential explicitly reads

$$H_C = \frac{La^2}{4} \sum_{\vec{b}} \int_0^L dz^- \int_0^L dy^- \sum_{p,q,n} \frac{G'_{\perp qp}(\vec{b}, z^-) G'_{\perp pq}(\vec{b}, y^-)}{[\pi n + (p-q)\varphi_{\vec{b}}]^2} e^{i2\pi n(z^- - y^-)/L}. \quad (5.1)$$

In order to separate possible singularities we work out the  $p, q$  sum:

$$\begin{aligned} H_C &= \frac{La^2}{4} \sum_{\vec{b}} \int_0^L dz^- \int_0^L dy^- \sum_{n \neq 0} \frac{G'_{\perp 11}(\vec{b}, z^-) G'_{\perp 11}(\vec{b}, y^-) + G'_{\perp 22}(\vec{b}, z^-) G'_{\perp 22}(\vec{b}, y^-)}{[\pi n]^2} e^{i2\pi n(z^- - y^-)/L} \\ &+ \frac{La^2}{4} \sum_{\vec{b}} \int_0^L dz^- \int_0^L dy^- \sum_n \frac{G'_{\perp 12}(\vec{b}, z^-) G'_{\perp 21}(\vec{b}, y^-)}{[\pi n + \varphi_{\vec{b}}]^2} e^{i2\pi n(z^- - y^-)/L} \\ &+ \frac{La^2}{4} \sum_{\vec{b}} \int_0^L dz^- \int_0^L dy^- \sum_n \frac{G'_{\perp 21}(\vec{b}, z^-) G'_{\perp 12}(\vec{b}, y^-)}{[\pi n - \varphi_{\vec{b}}]^2} e^{i2\pi n(z^- - y^-)/L}. \end{aligned} \quad (5.2)$$

Obviously the ‘abelian’ terms with  $G'_{11}$  and  $G'_{22}$  are infrared regular since  $n \neq 0$  in that case. The non-abelian terms can have singularities for  $\varphi \rightarrow 0, \pi$ . Exploiting the strong coupling basis, we show that these terms are also infrared regular. Such a ‘dynamical regularization’ is anticipated, because of the connection of the non-standard zero mode kinetic energy, the hermiticity defect, and the Coulomb term: the Jacobian vanishes at the points, where the ‘propagator’ becomes singular. Consider the last two terms in Eq. (5.2), which can be added using  $z \leftrightarrow y, n \leftrightarrow -n$ . This yields the non-abelian Coulomb contribution  $H_c$ :

$$H_c = \frac{La^2}{2} \sum_{\vec{b}} \int_0^L dz^- \int_0^L dy^- \sum_n \frac{G'_{\perp 21}(\vec{b}, z^-) G'_{\perp 12}(\vec{b}, y^-)}{(\pi n - \varphi_{\vec{b}})^2} e^{2\pi i n(z^- - y^-)/L}. \quad (5.3)$$

In this expression, we can identify the ‘Coulomb propagator’  $D_c(z^- - y^-, \varphi_{\vec{b}})$  in position space, and it can be evaluated with the result [22]

$$\begin{aligned} D_c(z^- - y^-, \varphi_{\vec{b}}) &\equiv \frac{L}{2} \sum_n \frac{e^{2\pi i n(z^- - y^-)/L}}{(\pi n - \varphi_{\vec{b}})^2} \\ &= e^{2i\varphi_{\vec{b}}(z^- - y^-)/L} \left[ \frac{L}{2 \sin^2 \varphi_{\vec{b}}} - |z^- - y^-| - i(z^- - y^-) \cot \varphi_{\vec{b}} \right] \\ &\equiv D_1 + D_2 + D_3. \end{aligned} \quad (5.4)$$

In the continuum limit one finds additional terms besides the linear propagator in one dimension. In the strong coupling approximation we integrate this Coulomb propagator and the off-diagonal  $G'_{\perp 21} G'_{\perp 12}$  with the Gegenbauer polynomials  $C_0(\varphi)$  over  $d\varphi J(\varphi)$  appropriate for the curvilinear coordinates. At this point it is evident that the Jacobian indeed prevents possible infrared singularities mentioned above.



Let us discuss the first term  $D_1$  in the Coulomb propagator. With the strong coupling ground state  $\Psi_{\{0\}}$  it leads to a Coulomb energy

$$\begin{aligned}
\langle \Psi_{\{0\}} | H_c^{(1)} | \Psi_{\{0\}} \rangle &= \langle \Psi_{\{0\}} | a^2 \sum_{\vec{b}} \int_0^L dz^- \int_0^L dy^- G'_{\perp 21}(\vec{b}, z^-) G'_{\perp 12}(\vec{b}, y^-) D_1 | \Psi_{\{0\}} \rangle \\
&= La^2 \sum_{\vec{b}} \int_0^L dz^- \int_0^L dy^- G'_{\perp 21}(\vec{b}, z^-) G'_{\perp 12}(\vec{b}, y^-) \times \\
&\quad \left\{ \frac{L}{2\pi i(z^- - y^-)} [e^{2\pi i(z^- - y^-)/L} - 1] \right\} \\
&\rightarrow La^2 \sum_{\vec{b}} |\tilde{Q}_{12}(\vec{b})|^2, \tag{5.5}
\end{aligned}$$

for large  $L$ , with

$$\tilde{Q}_{12}(\vec{b}) = \int_0^L dz^- G'_{\perp 12}(\vec{b}, z^-). \tag{5.6}$$

One sees that the expectation value of the off-diagonal ‘charge’  $\tilde{Q}_{12}(\vec{b})$  at each transverse site  $\vec{b}$  has to vanish in order to avoid an infinite Coulomb energy in the continuum limit

$$\langle \tilde{Q}_{12}(\vec{b}) \rangle \equiv 0 \quad \forall \vec{b}. \tag{5.7}$$

Recall that, in order to fully resolve Gauss’ Law, the third component of the global charge should vanish in the physical sector (cf. Eq. (2.17)). These two conditions together suggest that the physical states are real color singlets not merely color neutral states with a color three projection equal zero. The second term  $D_2$  of the Coulomb propagator gives a linearly rising potential in the  $L \rightarrow \infty$  limit,

$$\begin{aligned}
\langle \Psi_{\{0\}} | H_c^{(2)} | \Psi_{\{0\}} \rangle &= \langle \Psi_{\{0\}} | a^2 \sum_{\vec{b}} \int_0^L dz^- \int_0^L dy^- G'_{\perp 21}(\vec{b}, z^-) G'_{\perp 12}(\vec{b}, y^-) D_2 | \Psi_{\{0\}} \rangle \\
&\rightarrow -a^2 \sum_{\vec{b}} \int_0^L dz^- \int_0^L dy^- G'_{\perp 21}(\vec{b}, z^-) G'_{\perp 12}(\vec{b}, y^-) |z^- - y^-|. \tag{5.8}
\end{aligned}$$

Neglecting terms proportional to  $g$  with gluons in  $G'_{\perp 21}$  and only considering the external charges one gets a confining linear potential. Two color spin 1/2 point charges coupled to a color singlet at the same transverse site interact in longitudinal direction with the potential:

$$V_{12} = \frac{-1}{a^2} \frac{g^2}{4} \langle \vec{\tau}_1 \vec{\tau}_2 \rangle |z^- - y^-| = \frac{3}{4} g^2 |z^- - y^-| \frac{1}{a^2}. \tag{5.9}$$

The scale of the string tension is given in strong coupling by the lattice size  $a$  of the transverse lattice. In the continuum calculation it should be replaced by a correlation length generated in the transverse zero mode dynamics. The third term in the Coulomb propagator  $D_3$  does not contribute to the strong coupling ground state energy in the  $L \rightarrow \infty$  limit, since then  $\langle \tilde{Q}_{12}(\vec{b}) \rangle = 0$ .

One of the main advantages of the light front Coulomb gauge or axial gauges for QCD is visible here. Whereas in QED the Coulomb gauge is designed to give the  $1/r$  potential, the above gauge choices give confining potentials in zeroth order. Naturally, these potentials are linked to the choice of gauge, so one has to consider the perturbative corrections to the gauge potential. In axial gauge QED the potential for opposite charges has the form

$$M_1^{QED} = g^2 |z^- - y^-| \frac{1}{a^2}, \quad (5.10)$$

which appears to have the same confining properties as the QCD result. However, the first-order one photon exchange correction for soft photons with momenta  $(q_-, \vec{q}_\perp)$  has a spin independent contribution

$$M_2^{QED} = g^2 \frac{\vec{q}_\perp^2}{q_- q_-} \frac{\theta(q_-)}{q_-} \frac{-1}{\vec{q}_\perp^2/q_-}. \quad (5.11)$$

After transforming  $M_2^{QED}$  to coordinate space, it is seen that this one-photon exchange cancels the confining gauge artifact and the Coulomb potential  $1/r$  plus spin dependent corrections remain.

In QCD the one-gluon exchange contributions have to be discussed separately for color charged gluons  $A_\perp^{1,2}(x^-, x_\perp)$  and color neutral gluons. The  $A_\perp^{1,2}$  components of the transverse gluon fields interact with the zero mode  $a_-^3(x_\perp)$  fields. These ‘background fields’ have non-zero expectation values in the strong coupling limit for  $g_{\text{eff}}$ . In this way the  $A_\perp^{1,2}$  fields may acquire a mass. In other words, we argue that the dispersion relation of transverse colored gluons possibly is changed to

$$k_+ = \frac{1}{\eta^2} \left( -k_- + \sqrt{k_-^2 + \eta^2(k_\perp^2 + \frac{4}{\eta^2} \langle \varphi^2 \rangle / L^2)} \right). \quad (5.12)$$

Consequently, the one-gluon exchange can no longer cancel the linear confinement potential at large distances, as the fields are now massive and thus finite-range.

Our approach produces similar results as the similarity transformation scheme [6,23]. This scheme has been proposed by Glazek and Wilson [24] for the light front Hamiltonian and by Wegner [25] independently for condensed matter physics. It avoids vanishing energy denominators for the  $q_- \rightarrow 0$  region for one-gluon exchange by a cutoff  $\lambda$ . In higher orders the region of validity for  $q_-$  can be enlarged successively (the cutoff  $\lambda$  can be made smaller). In our approach near the light front we can give the physical origin of the cutoff  $\lambda$ . It lies in the zero mode fields  $a_-(x_\perp)$  which limit the long-range propagation of gluon fields. We only use the strong coupling approximation for the ground state wave functional of the transverse zero mode lattice. Certainly higher orders and a more accurate description of the zero mode dynamics are necessary to prove that the linear confinement potential is preserved. Color neutral gluon fields  $A_\perp^{3'}(x^-, x_\perp)$  do not directly interact with  $a_\perp^3(x_\perp)$ , but by their construction in Eq. (2.16) their two-dimensional longitudinal zero modes ( $q_- = 0$ ) have been subtracted. The corresponding two-dimensional transverse parts, however, are still present as dynamical modes.

It is more complicated to analyze two color charges separated in transverse direction. Consider two color charges separated by  $x_\perp$  and oriented along the color 3-direction. As color 3-charges they experience the two-dimensional Coulomb potential via the electric field

$$e_\perp^3(x_\perp) = g\nabla_\perp \int dy^- dy_\perp d(x_\perp - y_\perp) \rho_m^3(y^-, y_\perp). \quad (5.13)$$

The above propagator generates a logarithmic potential, which is also confining. This potential is unaffected by the zero modes  $a_-$ , since the strong coupling ground state expectation value of  $\nabla_\perp a_-$  vanishes. Explicitly, we obtain

$$V_{12} = \frac{g^2}{a^2 M^2 L} \frac{\tau_1^3 \tau_2^3}{4} \ln \left| \frac{x_\perp - y_\perp}{a} \right|. \quad (5.14)$$

It corresponds to spreading flux lines in 2 dimensions and strongly violates the rotational invariance in the spatial coordinates. To investigate this problem further, one must under-

stand the role played by the zero modes in the continuum limit. Work in this direction is in progress [26].

## VI. SUMMARY

We have presented a near light front description of QCD. In our Hamiltonian approach, formulated in a finite volume, the modified light-cone gauge  $\partial_- A_- = 0$  is a natural choice. The resulting asymmetric treatment of transverse and longitudinal dynamics matches the physics of deep inelastic scattering where large momenta of the hadron are involved. We argue that the well-known physical appeal of an infinite momentum frame can indeed be realized rather naturally in near light front coordinates.

In the chosen canonical formulation, Gauss' law appears as a quantum mechanical constraint to be implemented on physical states. It reflects the presence of redundant gauge variables. Using unitary gauge fixing transformations, these are eliminated by implementing Gauss' law. The result is a Hamiltonian formulated in terms of unconstrained dynamical variables.

This Hamiltonian contains zero mode degrees of freedom, which only depend on transverse coordinates. The zero-mode dynamics apparently generates the dominant non-perturbative physics with interesting implications. In the strong coupling limit,  $g_{\text{eff}}^2 = \frac{g^2 LM}{4\sqrt{2}} \gg 1$ , the energy gaps between excited 'gluonic' states and the ground state are large – in contrast to QED. Another indication of confinement is a linear quark-quark potential in longitudinal direction, which is not merely a gauge artifact – as it is in QED. In transverse direction confinement is supported via a logarithmic quark-quark potential. One has yet to discover how the two-dimensional dynamics relates to the full-three dimensional dynamics.

The eigenfunctions of the zero mode Hamiltonian in the weak coupling limit are spin waves. We also have investigated the intermediate coupling regime by means of a cluster expansion. Via an effective Hamiltonian method the two-site energy was explicitly calculated for the entire range of couplings. We demonstrated that the results indeed converge to the

analytical expressions for  $g_{\text{eff}}^2 \gg 1$  and  $g_{\text{eff}}^2 \ll 1$ . The spectra of  $N$ -sites can be constructed in the ‘low density’ approximation.

Our approach opens a potential path to construct constituent quark models on the light front by eliminating the negative energy solutions from the near light front Hamiltonian. The effective Hamiltonian method utilized here for the zero modes may also be the appropriate tool to study the mechanism of chiral symmetry breaking.

### APPENDIX: $SU(N)$ HAMILTONIAN INCLUDING FERMIONS

The resolution of the Gauss law constraint via ‘unitary gauge fixing transformations’ can also be achieved in the  $SU(N)$ -case, including dynamical fermions [10,11]. The final Hamiltonian in near light front coordinates is formulated in terms of the following  $SU(N)$  variables:

- Fermion fields  $\psi$  and  $\psi^\dagger$ , obeying standard anti-commutation relations. (The  $N$  color indices, as well as Dirac and flavor labels are suppressed.) It should be emphasized that  $\psi_- = \frac{1}{2}(1 - \alpha^3)\psi$  is a dynamical field, whereas on the exact light-front it is constrained.
- Transverse gluon fields,  $A_i^a(i = 1, 2; a = 1, \dots, N^2 - 1)$ , without the neutral, two-dimensional, longitudinal parts, which have been eliminated. This means that

$$\partial_i \int_0^L dx^- A_i^{\prime c_0}(\vec{x}_\perp, x^-) = 0, \quad (\text{A.1})$$

where the color index with subindex ‘0’ refers to the Cartan subalgebra. In the usual representation this corresponds to diagonal  $\lambda$ -matrices. The conjugate chromoelectric fields are denoted with  $\Pi_i^a$ .

- Zero mode gluon fields  $a_-$  and their canonical momenta  $p_-$ . Neither of these fields depend on  $x^-$  and both are color diagonal. Thus one can write

$$\begin{aligned}
a_-(\vec{x}_\perp) &= \sum_{c_0=1}^{N-1} a_-^{c_0}(\vec{x}_\perp) \frac{\lambda^{c_0}}{2}, \\
p_-(\vec{x}_\perp) &= \sum_{c_0=1}^{N-1} p_-^{c_0}(\vec{x}_\perp) \frac{\lambda^{c_0}}{2}.
\end{aligned} \tag{A.2}$$

The Hamiltonian density in the physical Hilbert space explicitly reads

$$\begin{aligned}
\mathcal{H} &= -i \frac{2}{\eta^2} \psi_\perp^\dagger (\partial_- - ig a_-) \psi_- - i \frac{1}{\eta} \psi_\perp^\dagger \vec{\alpha}_\perp (\vec{\nabla}_\perp - ig \vec{A}'_\perp) \psi + m \frac{1}{\eta} \psi_\perp^\dagger \beta \psi \\
&+ \text{tr} [\partial_1 A'_2 - \partial_2 A'_1 - ig [A'_1, A'_2]]^2 + \frac{1}{\eta^2} \text{tr} [\Pi'_\perp - (\partial_- \vec{A}'_\perp - ig [a_-, \vec{A}'_\perp])]^2 \\
&+ \frac{1}{\eta^2} \text{tr} \left[ \frac{1}{L} \vec{e}_\perp - \nabla_\perp a_- \right]^2 + \frac{1}{2L^2} \sum_{c_0} p_-^{c_0 \dagger}(\vec{x}_\perp) p_-^{c_0}(\vec{x}_\perp) \\
&+ \frac{1}{L^2} \int_0^L dz^- \int_0^L dy^- \sum_{p,q,n} ' \frac{G'_{\perp qp}(\vec{x}_\perp, z^-) G'_{\perp pq}(\vec{x}_\perp, y^-)}{\left[ \frac{2\pi n}{L} + g(a_{-,q}(\vec{x}_\perp) - a_{-,p}(\vec{x}_\perp)) \right]^2} e^{i2\pi n(z^- - y^-)/L},
\end{aligned} \tag{A.3}$$

with  $p, q = 1, \dots, N$ . The operator  $G'_\perp$ , the neutral chromo-electric fields  $\vec{e}_\perp$ , and the neutral charge  $Q^{c_0}$ , which appears below, are defined as the generalizations of the corresponding quantities in the main text. Note that the matter density contains the dynamical fermion fields,

$$\rho_m^a(\vec{x}_\perp, x^-) = \psi^\dagger(\vec{x}_\perp, x^-) \frac{\lambda^a}{2} \psi(\vec{x}_\perp, x^-). \tag{A.4}$$

The variables defined above are not constrained apart from the global conditions

$$Q^{c_0} |\Phi'\rangle = 0. \tag{A.5}$$

The neutral components of the total color-charge vanish in the sector of (transformed) physical states. This completes the  $SU(N)$  formulation of axial gauge light cone QCD.

## REFERENCES

- [1] J. D. Bjorken, J. B. Kogut, and D. E. Soper, Phys. Rev. D **3**, 1382 (1971).
- [2] J. B. Kogut and L. Susskind, Phys. Rep. C **8**, 75 (1973).
- [3] H. C. Pauli and S. J. Brodsky, Phys. Rev. D **32**, 1993 (1987).
- [4] E. V. Prokhvatilov and V. A. Franke, Sov. J. Nucl. Phys. **49**, 688 (1989).
- [5] F. Lenz, M. Thies, S. Levit, and K. Yazaki, Ann. Phys. (N.Y.) **208**, 1 (1991).
- [6] K. G. Wilson, T. S. Walhout, A. Harindranath, W. M. Zhang, R. J. Perry, and S. D. Glazek, Phys. Rev. D **49**, 6720 (1994).
- [7] E. V. Prokhvatilov, H. W. L. Naus, and H. J. Pirner, Phys. Rev. D **51**, 2933 (1995).
- [8] J. P. Vary, T. J. Fields, and H. J. Pirner, Phys. Rev. D **53**, 7231 (1996).
- [9] F. Lenz, H. W. L. Naus, K. Ohta, and M. Thies, Ann. Phys. (N.Y.) **233**, 17 (1994).
- [10] F. Lenz, H. W. L. Naus, and M. Thies, Ann. Phys. (N.Y.) **233**, 317 (1994).
- [11] F. Lenz, H. W. L. Naus, and M. Thies, private communication.
- [12] M. Thies, Talk presented at the International School of Nuclear Physics *Quarks in Hadrons and Nuclei*, Erice, 1995, hep-ph/9511450.
- [13] H. Griesshammer, in *Nonperturbative Approaches to Quantum Chromodynamics*, Proceedings of the International Workshop, Trento, 1995, edited by D. Diakonov, p. 24.
- [14] J. Przeszowski, H. W. L. Naus, and A. C. Kalloniatis, Phys. Rev. D **54**, 5135 (1996).
- [15] F. Lenz, E. J. Moniz, and M. Thies, Ann. Phys. (N.Y.) **242**, 429 (1995).
- [16] T. J. Fields, Ph.D. thesis, Iowa State University, 1996.
- [17] J. B. Bronzan, Phys. Rev. D **37**, 1621 (1988).
- [18] S. V. Shabanov, Phys. Lett. B **318**, 323 (1993).

- [19] C. J. Morningstar and M. Weinstein, Phys. Rev. D **54**, 4131 (1996).
- [20] T. J. Fields, J. P. Vary, and K. S. Gupta, Mod. Phys. Lett. **A11**, 2233 (1996).
- [21] D. C. Zheng, J. P. Vary, and B. R. Barrett, Nucl. Phys. **A560**, 211 (1993).
- [22] M. Engelhardt and B. Schreiber, Z. Phys. A **351**, 71 (1995).
- [23] R. J. Perry, Lectures given at Hadrons 94 Workshop, Gramado, Brazil, hep-th/9407056.
- [24] S. D. Glazek and K. G. Wilson, Phys. Rev. D **49**, 4214 (1994).
- [25] F. Wegner, Ann. Physik (Leipzig) **3**, 77 (1994).
- [26] H. J. Pirner, work in progress.



# FIGURES

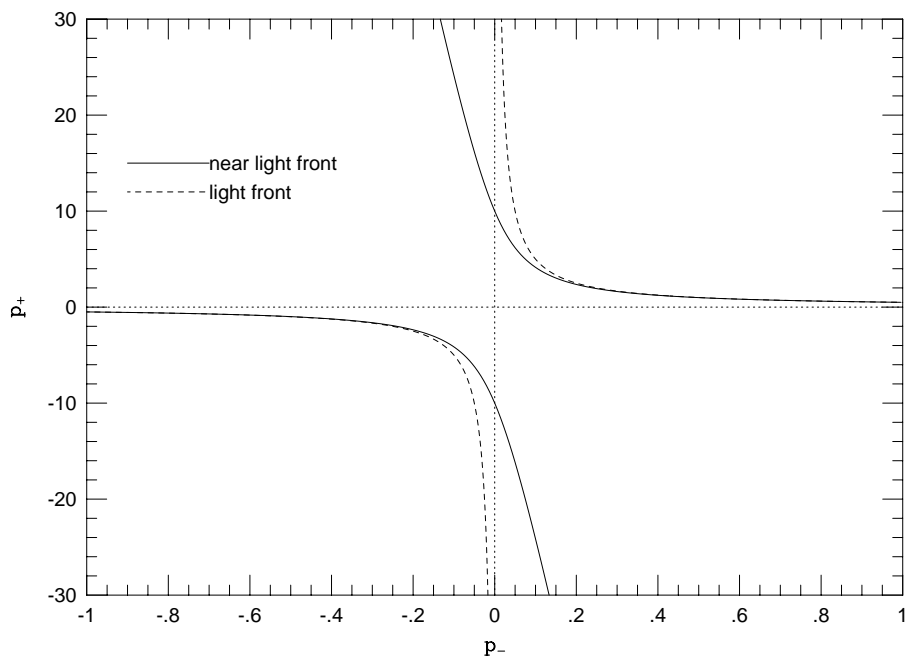


FIG. 1. Dispersion relations in the near light front coordinate system and directly on the light front.

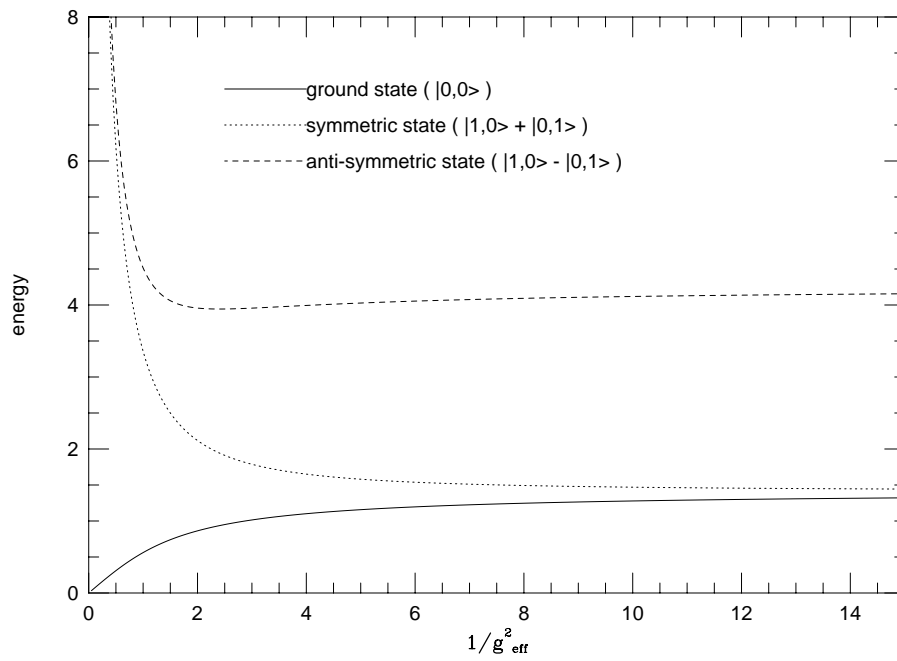


FIG. 2. Energies of first 3 states in the zero mode sector calculated via effective Hamiltonian method.